

Comparison of Pressure-Strain Correlation Models for the Flow Behind a Disk

R. S. Amano*

University of Wisconsin, Milwaukee, Wisconsin

Introduction

THIS Note reports the behavior of Reynolds stresses in the separated wake region behind a disk that is attached in a normal fashion to a long cylinder with a smaller diameter. Such separated turbulent flows are common flow phenomena observed in many industrial problems. It is important to understand the mechanism of energy transfer that occurs among the Reynolds-stress components in order to improve prediction of turbulence levels.

The recent development of computer techniques for solving the partial-differential equations governing these flows has made theoretical studies easier and less costly by eliminating the need for extensive experimental work during the design stages.

In this Note, computations of the turbulent flow were made in the region beyond a disk by employing the second-order closure model of turbulence. The results were compared with the existing experimental data at several streamwise locations.

Particular attention was paid to evaluation of the pressure-strain correlation of the Reynolds stresses, which plays an important role in estimating turbulence-energy transfer among stress components in the separated shear flow region. First, the models of Naot et al.^{1,2} and Launder et al.³ were examined and, then, the results computed using these models were compared with existing experimental data. Moreover, a simpler model was formulated that provides better profiles of the Reynolds stresses in the wake region.

Formulation of the Pressure-Strain Correlations

The set of differential equations governing the transport of the kinematic Reynolds stresses $-\overline{u_i u_j}$ can be written in the form

$$\begin{aligned} (U_k \overline{u_i u_j})_{,k} = & -(\overline{u_j u_k} U_{i,k} + \overline{u_i u_k} U_{j,k}) - 2\nu \overline{u_{i,k} u_{j,k}} \\ & + (\overline{p/\rho})(u_{i,j} + u_{j,i}) - [\overline{u_i u_j u_k} - \nu(\overline{u_i u_j})_{,k} \\ & + (\overline{p/\rho})(\delta_{jk} u_i + \delta_{ik} u_j)]_{,k} \end{aligned} \quad (1)$$

where u and U represent turbulent fluctuating and mean velocities, respectively, and p denotes the fluctuating pressure.

To close Eq. (1) in terms of mean velocities and Reynolds stresses, the turbulence quantities on the right-hand side of Eq. (1) must be represented as empirical functions of the mean velocities and Reynolds stresses and their derivatives.

Here attention was focused on the pressure-strain correlation on the third term of the right-hand side of Eq. (1). Several models have been proposed for the pressure-strain correlations, but these have been tested only for relatively simple flows such as free shear flows and boundary layers. To date, these have not yet been extensively tested for the recirculating flows. Herein, several models have been employed to compute all turbulent kinematic stress components.

Model 1: Naot et al.¹

$$(\overline{p/\rho})(u_{i,j} + u_{j,i}) = -C_\phi (G_{ij} - \frac{2}{3}\delta_{ij}G) + \phi \quad (2)$$

Model 2: Naot et al.²

$$\begin{aligned} (\overline{p/\rho})(u_{i,j} + u_{j,i}) = & -a_1 (G_{ij} - \frac{2}{3}\delta_{ij}G) \\ & + a_2 (H_{ij} - \frac{2}{3}\delta_{ij}G) + a_3 k (U_{i,j} + U_{j,i}) + \phi \end{aligned} \quad (3)$$

Model 3: Launder et al.³

$$\begin{aligned} (\overline{p/\rho})(u_{i,j} + u_{j,i}) = & -a_4 (G_{ij} - \frac{2}{3}\delta_{ij}G) \\ & -a_5 (H_{ij} - \frac{2}{3}\delta_{ij}G) - a_6 k (U_{i,j} + U_{j,i}) + \phi \end{aligned} \quad (4)$$

where

$$G = -\overline{u_i u_j} U_{i,j} \quad (5)$$

$$G_{ij} = -(\overline{u_i u_k} U_{j,k} + \overline{u_j u_k} U_{i,k}) \quad (6)$$

$$H_{ij} = -(\overline{u_i u_k} U_{k,j} + \overline{u_j u_k} U_{k,i}) \quad (7)$$

$$\phi = -1.5(\epsilon/k)(\overline{u_i u_j} - \frac{2}{3}\delta_{ij}k) \quad (8)$$

and where $C = 1.5$.

The coefficients used above are given as

$$a_1 = (76 - 8b_1)/105, \quad a_2 = (22 + 64b_1)/105$$

$$a_3 = 2(9 + 72b_1)/315, \quad a_4 = (b_2 + 8)/11$$

$$a_5 = (8b_2 - 2)/11, \quad a_6 = (30b_2 - 2)/55$$

The first model was developed by removing the isotropic constraint from the double-velocity, two-point correlation tensor. The second model, an extension of the first, was proposed in terms of the single-point tensor and three arbitrary functions of the absolute value of the two-point separation distance.

The third model was obtained by approximating the pressure-strain correlation by an arbitrary fourth-order tensor, where the single-point, double-velocity correlations were used.

Results and Discussion

Figure 1 shows the axial velocity profiles at several different locations behind the disk with a diameter D_d , which is attached to a $1/6D_d$ diameter cylinder. The radial coordinate is normalized by the disk radius R . Agreement between computed results and the experimental data of Smyth⁴ is very

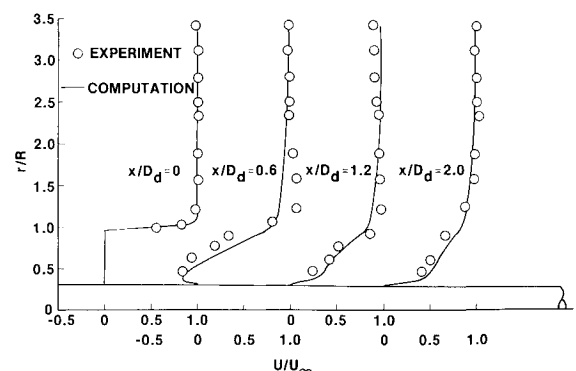


Fig. 1 Mean velocity profiles behind a disk.

Received June 17, 1985; revision submitted March 14, 1986. Copyright © American Institute of Aeronautics and Astronautics, Inc., 1986. All rights reserved.

*Associate Professor, Mechanical Engineering Department. Member AIAA.

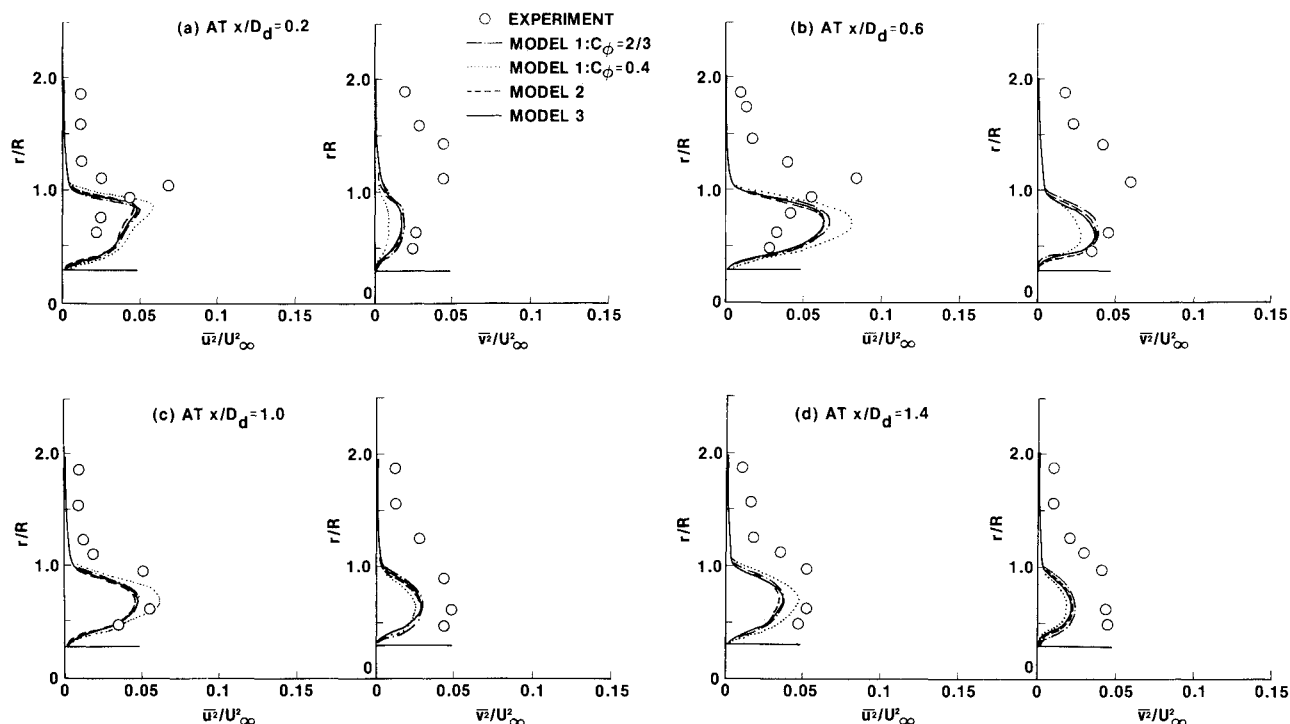


Fig. 2 Reynolds-stress profiles behind a disk (using different models).

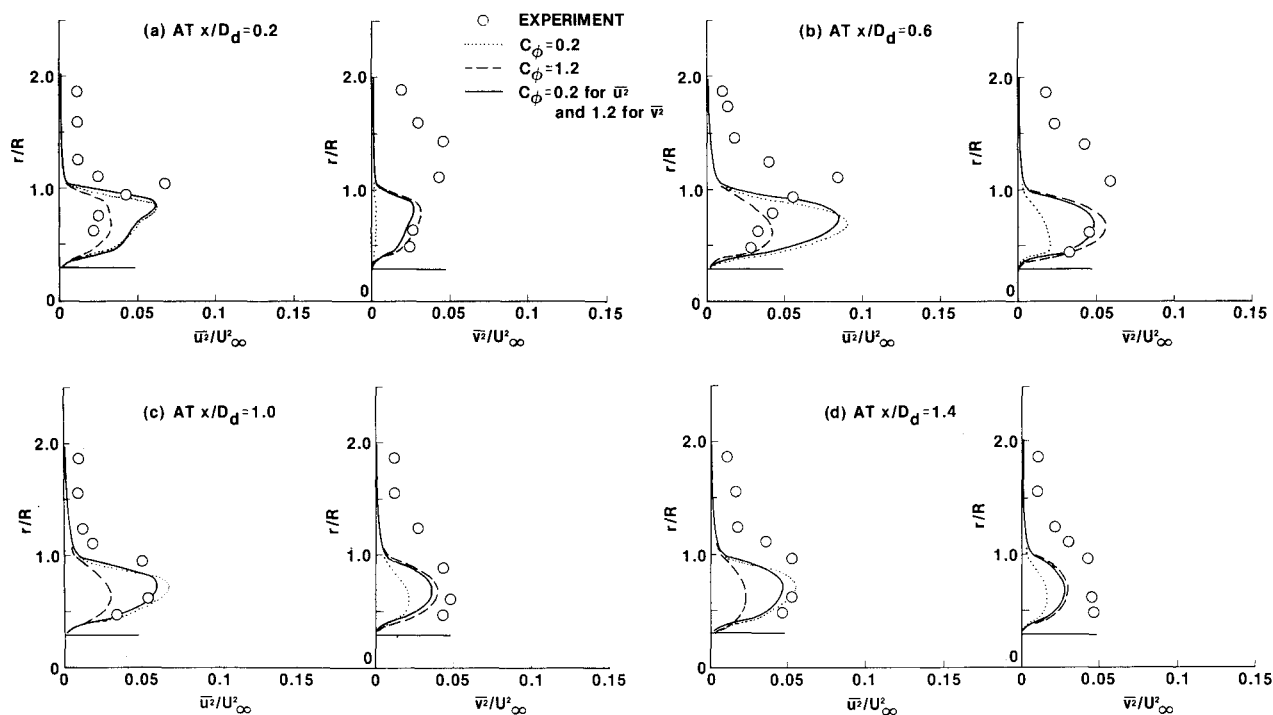


Fig. 3 Reynolds-stress profiles behind a disk (using different coefficients).

good (within 15% discrepancy). It was also discerned that the velocity profiles were almost independent of the pressure-strain correlation although the computed velocity profiles using all the models are not shown in the figure.

Figure 2 shows the normal stress profiles of $\overline{u^2}$ and $\overline{v^2}$ at four different locations downstream of the disk. The computations were made by using models 1, 2, and 3, and the results were compared with the experimental data.⁴ When the coefficient $C_\phi = 2/3$, which was originally used by Naot et al.,¹ is used for model 1, the results are all similar to each

other. This is mainly because, although all the models are derived differently, their final forms are very close. In particular, models 2 and 3 have almost the same values for the coefficient of the first term on the right-hand side of Eqs. (3) and (4). Naot et al.² obtained the value of -0.5 for the coefficient b_1 , and Launder et al.³ chose the value of 0.4 for b_2 , which results in $a_1 \approx a_4 \approx 0.76$. Also, it is observed that the second and third terms of models 2 and 3 have a minor influence on the levels of turbulence stresses; thus, the pressure-strain correlation may be represented by the first

term alone. Note that model 1 has this term only.

In Fig. 2, the computed results using model 1 with $C_\phi = 0.4$ are also shown. This value was recommended by Launder et al.³ in reference to equilibrium shear flows. The computed results using the coefficient $C_\phi = 0.4$ show that the levels of $\overline{u^2}$ increase about 20%, while those of $\overline{v^2}$ decrease about the same amount; this indicates that the redistributive action is reduced about 20% by changing C_ϕ from 0.667 to 0.4. Therefore, the turbulence energy created due to mean strain of the mainstream flow $\overline{u^2}$ is not transferred completely to the normal components $\overline{v^2}$ and $\overline{w^2}$ of the turbulence stresses.

It was generally observed that all the models underpredict the levels of the Reynolds stresses by 10–50%. In order to predict the Reynolds stresses more accurately in recirculating flows, the original models tested for equilibrium shear flows need to be revised. For ease of analysis, model 1 was chosen to refine prediction of the turbulence level. Two computations were performed by using values of 0.2 and 1.2 for C_ϕ . The results are shown in Fig. 3. As depicted in this figure, the small value of coefficient C_ϕ results in appropriate levels of $\overline{u^2}$ but unacceptably low levels of $\overline{v^2}$. On the other hand, the large value of C_ϕ gives reversed results; that is, the levels of $\overline{v^2}$ are substantial but those of $\overline{u^2}$ are too low.

When the flow reattaches to the center cylinder, the flow starts accelerating in the downstream direction, which causes a high mean normal strain as the flow recovers. Thus, the term with $\overline{u^2} \partial U_1 / \partial x_1$ in the pressure-strain correlation in the $\overline{u^2}$ equation becomes higher than those in the fully developed flows, which results in significant energy transfer from $\overline{u^2}$ to $\overline{v^2}$. This effect must be suppressed to some extent in the present flow situation, whereas the corresponding component, which balances the energy level of $\overline{v^2}$, is relatively small. Therefore, the redistributive action in the $\overline{v^2}$ equation needs to be promoted more.

For the reasons discussed above, the cases in which the coefficient C_ϕ for $\overline{u^2}$ was decreased to 0.2 and in which coefficient C_ϕ for $\overline{v^2}$ was raised to 1.2 is demonstrated in the same figure. The results obtained with this treatment show much improvement, as indicated in Fig. 3. This observation suggests that the coefficients of the isotropic generation rates for the Reynolds stresses [i.e., the first terms of Eqs. (4–6)] should be adjusted by their values by the effect of the mean strains since the flow patterns are strongly affected by the mean strains. The strain variations are particularly complex in the reattaching shear layers being accompanied by the recirculating flows. In this way the Reynolds stresses can be more accurately evaluated by using such simpler formulations.

Conclusions

The models by Naot et al. and Launder et al. effectively give similar results, and both models are reasonably reliable. The energy redistribution can be improved for reattaching shear flows by taking into account the effects of mean strain.

Acknowledgment

This study was sponsored by NASA Lewis Research Center under Grant NAG 3-546.

References

- Naot, D., Shavit, A., and Wolfshtein, M., "Interaction Between Components of the Turbulent Velocity Correlation Tensor Due to Pressure Fluctuations," *Israel Journal of Technology*, Vol. 8, No. 3, 1970, pp. 259–269.
- Naot, D., Shavit, A., and Wolfshtein, M., "Two-Point Correlation Model and the Redistribution of Reynolds Stresses," *The Physics of Fluids*, Vol. 16, No. 6, 1973, pp. 738–743.
- Launder, B. E., Reece, G. J., and Rodi, W., "Progress in the Development of Reynolds-Stress Turbulence Closure," *Journal of Fluid Mechanics*, Vol. 68, Part 3, 1975, pp. 537–566.
- Smyth, R., "Turbulent Flow Over a Disk Normal to a Wall," *ASME Journal of Fluids Engineering*, Vol. 101, 1979, pp. 461–465.

Reverse Flow Radius in Vortex Chambers

G. H. Vatistas,* S. Lin,† and C. K. Kwok†
Concordia University, Montreal, Canada

Nomenclature

A_{in}	= total inlet area
P	= static pressure
Q	= inlet volumetric flow rate
Q_r	= volumetric flow rate of the reverse flow
R_{CF}	= core radius (radius of maximum tangential velocity)
R_E	= exit port radius
R_r	= reverse flow radius
R_0	= radius of the main chamber
V_r, V_θ, V_z	= radial, tangential, and axial velocity components, respectively
Γ	= strength of the vortex
φ	= angle between total velocity vector and tangential velocity component at the inlet

Subscripts

in, F	= properties evaluated at the inlet and on the exit plane, respectively
-------	---

Introduction

It is well known that when sufficiently large swirl is applied at the inlet of a vortex chamber, the resulting vortex breakdown at the centrally located outlet port is accompanied by a strong reverse flow near the axis of rotation. Recently, it has been experimentally demonstrated that a significant reduction in static pressure drop across the chamber (inlet to outlet) can be obtained by plugging the exit flow.¹ In the present Note, the dimensionless reverse flow radius is determined based on the equations of motion and energy. The reverse flow radius is shown to depend solely on geometrical parameters of the vortex chamber.

Analysis

From the experimental results of Kwok,² it can be seen that the static pressure outside the core radius R_{CF} is approximately equal to the ambient (P_a). Inside the core, the static pressure decreases noticeably. Close to the axis of symmetry, the parabolic profile of the pressure suggests a strong influence of the pressure by the solid body rotation. If a funnel-like flow entrainment is assumed to take place, the reverse flowfield must resemble that of Fig. 1. At $z=0$, the radial velocity component will be approximately zero while a large average axial velocity component must be present. If the static pressure at $r=R_{CF}$ is P_a , it will be below the ambient in the interval $(0, R_{CF})$. From the radial momentum equation,

$$P_F(r) = (\rho m^2 / 2) (r^2 - R_{CF}^2) + P_a \quad (1)$$

where

$$m = \Gamma / 2\pi R_{CF}^2$$

Presented as Paper 84-1548 at the AIAA 17th Fluid Dynamics, Plasmadynamics, and Lasers Conference, Snowmass, CO, June 25–27, 1984; received Jan. 22, 1985; revision received Feb. 25, 1986. Copyright © American Institute of Aeronautics and Astronautics, Inc., 1986. All rights reserved.

*Assistant Professor, Department of Mechanical Engineering, Member AIAA.

†Professor of Engineering, Department of Mechanical Engineering.